PAPER

Temperature-dependent mechanical properties and the microscopic deformation mechanism of bilayer γ-graphdiyne under tension

Temperature-dependent mechanical properties and the microscopic deformation mechanism of bilayer γ-graphdiyne under tension

Bo Song[1,2] , **Bolin Yang**[1,2], **Cun Zhang**[3,4,*], **Chao Wang**[5] and **Shaohua Chen**[1,2,*]

[1] Institute of Advanced Structure Technology, Beijing Institute of Technology, Beijing 100081, People's Republic of China
[2] Beijing Key Laboratory of Lightweight Multi-functional Composite Materials and Structures, Beijing Institute of Technology, Beijing 100081, People's Republic of China
[3] Department of Engineering Mechanics, Shijiazhuang Tiedao University, Shijiazhuang 050043, People's Republic of China
[4] Hebei Key Laboratory of Smart Materials and Structures Mechanics, Shijiazhuang Tiedao University, Shijiazhuang 050043, People's Republic of China
[5] LNM, Institute of Mechanics, Chinese Academy of Sciences, Beijing 100190, People's Republic of China

E-mail: zhangcun@stdu.edu.cn, shchen@bit.edu.cn and chenshaohua72@hotmail.com

CrossMark

Abstract

γ-graphdiyne (γ-GDY) is a new two-dimensional carbon allotrope that has received increasing attention in scientific and engineering fields. The mechanical properties of γ-GDY should be thoroughly understood for realizing their practical applications. Although γ-GDY is synthesized and employed mainly in their bilayer or multilayer forms, previous theoretical studies mainly focused on the single-layer form. To evaluate the characteristics of the multilayer form, the mechanical properties of the bilayer γ-GDY (γ-BGDY) were tested under uniaxial tension using the molecular dynamics simulations. The stress–strain relation of γ-BGDY is highly temperature-dependent and exhibits a brittle-to-ductile transition with increasing temperature. When the temperature is below the critical brittle-to-ductile transition temperature, γ-BGDY cracks in a brittle manner and the fracture strain decreases with increasing temperature. Otherwise, it exhibits ductile characteristics and the fracture strain increases with temperature. Such a temperature-dependent brittle-to-ductile transition is attributed to the interlayer cooperative deformation mechanism, in which the co-rearrangement of neighboring layers is dominated by thermal vibrations of carbon atoms in diacetylenic chains. Furthermore, the brittle-to-ductile transition behavior of γ-BGDY is independent of loading direction and loading rate. The ultimate stress and Young's modulus decrease at higher temperatures. These results are beneficial for the design of advanced γ-GDY-based devices.

Supplementary material for this article is available online

Keywords: bilayer γ-graphdiyne, mechanical properties, brittle-to-ductile transition, microscopic deformation mechanism, molecular dynamics

(Some figures may appear in colour only in the online journal)

---

* Authors to whom any correspondence should be addressed.

1. Introduction

As a new series of two-dimensional carbon allotropes, graphynes are constructed by replacing a portion of aromatic C–C bonds in graphene with acetylenic linkages with single and triple bonds [1]. Depending on the replacement ratio, graphynes can have unlimited geometrical configurations and are typically divided into three types: α-, β-, and γ-graphynes [2, 3]. Particularly, γ-graphdiyne (γ-GDY) was the first graphyne material to be successfully synthesized in the laboratory [4]. Benefiting from excellent characteristics that are even superior to graphene, such as numerous highly reactive sites [5], a uniform nanoscale pore structure [2], and an intrinsic nonzero bandgap [6, 7], γ-GDY holds great potential in various applications, such as lithium-ion batteries [8], energy conversion and storage [9, 10], catalysis [11, 12], water desalination and gas separation [13], and nanoelectronics [14].

To guarantee the service performance of γ-GDY in the aforementioned applications, a comprehensive understanding of the mechanical behavior of γ-GDY under specific loading conditions is crucial. Recently, theoretical studies mainly focused on the mechanical properties of the single-layer γ-GDY (γ-SGDY) [15, 16]. Employing molecular dynamics (MD) simulations, Cranford *et al* [17] investigated the directionally dependent tensile properties of γ-SGDY. They have indicated that the ultimate strength of γ-SGDY is 36.0 and 45.5 GPa along the armchair and zigzag directions, respectively. According to the density functional theory (DFT) calculations, Pei [6] proposed that the in-plane stiffness and the Poisson's ratio of γ-SGDY are 7.60 eV/$\mathring{A}^2$ and 0.453, respectively. Hou *et al* [16] built an analytical molecular mechanics model of γ-SGDY and provided closed-form expressions for the in-plane stiffness and Poisson's ratio. Georgantzinos and Siampanis [18] determined the size-dependent elastic properties of γ-SGDY by conducting a finite element investigation.

However, compared to the γ-SGDY, the multilayer γ-GDY is more commonly synthesized and applied in experimental works and practical applications [4, 11, 19]. It is also well known that the layer number plays an important role in tuning the performance of multilayer γ-GDY. For example, in comparison with the γ-SGDY, the bilayer and trilayer γ-GDY are reported to possess better electronic properties (e.g. a more tunable bandgap) and have a higher application value in nanoelectronics [7]. Researchers also studied the effect of the layer number on the mechanical performance of γ-GDY. Using MD simulations, Rouhi *et al* [20] proposed that Young's modulus of multilayer γ-GDY is directionally dependent and its fracture stress and strain are inversely related to the layer number. Xiao *et al* [19] conducted nanoindentation experiments on multilayer γ-GDY films with an atomic force microscope, and the measured value of the elastic modulus is 50% less than that in their MD simulations. According to their speculation, this phenomenon was most likely induced by the difference in layer number and defects in the sample; however, no further experimental or numerical evidence was provided. In other words, how the layer number of γ-GDY affects its mechanical properties remains unclear.

Besides, our recent study revealed that temperature can considerably affect the mechanical performance of a multilayer α-graphyne nanoscroll, inducing a brittle-ductile transition under uniaxial tension [21]. Ahangari [22] found that the in-plane stiffness and Young's modulus of γ-SGDY greatly decrease at high temperatures. Using MD simulations, Ma *et al* [23] showed that the high-temperature behavior of γ-SGDY is far less stable than that of graphene. However, the explicit effect of temperature on the mechanical properties of multilayer γ-GDY remains undetermined.

In the present work, the bilayer γ-GDY (γ-BGDY) was considered to test its mechanical properties under uniaxial tension using the MD method, in which the effects of temperature, loading direction, and loading rate were considered. This study should help the design of advanced γ-GDY-based devices in practical applications.

2. Numerical model and methodology

Figures 1(a), (b) shows the simulation model of the γ-BGDY sheet in a typical AB stack type, which is approximately a square with a side length of approximately 15 nm. Periodic boundary conditions were applied along the *x*- and *y*-directions to avoid the edge effects and a free boundary condition was applied along the *z*-direction. Three types of carbon bonds in γ-GDY, including aromatic, single, and triple bonds, are illustrated in figure 1(c). Notably, the carbon atoms on the diacetylenic chains are sp^1-hybridized and have a high chemical activity [2, 23]. According to previous experimental measurements [24], AB stacking with a parallel displacement of 0.546 nm along the *x*-direction was adopted for L1 and L2 in this study (figure 1(d)).

Uniaxial stretching tests of the γ-BGDY shown in figure 1 were fulfilled using the MD simulation approach, as implemented in the open-source code large-scale atomic/molecular massively parallel simulator (LAMMPS) [25]. The interaction between the carbon atoms was described by the adaptive intermolecular reactive empirical bond order (AIREBO) potential [26], which can accurately reproduce the formation and breakage of C–C bonds and has been widely used to evaluate the mechanical properties of carbon allotropes, such as carbon nanotubes [27, 28], graphene [29, 30], diamond [31], diamondene [32, 33], and graphynes [21, 34, 35]. The feasibility and reliability of AIREBO potential in simulating the mechanical property of carbon nanomaterials have also been confirmed by DFT calculations [21, 35, 36] and experiment results [37]. Similar to previous studies [21, 35], to avoid spuriously high bond forces and nonphysical results near the fracture region, a cutoff distance of 2.0 Å was adopted for the covalent interaction in the AIREBO potential [38].

For all simulations, the tensile deformation was realized by changing the length of the simulation box along the loading direction at a constant engineering strain rate. When a constant tensile strain rate of $\dot{\varepsilon}$ was adopted, the current length
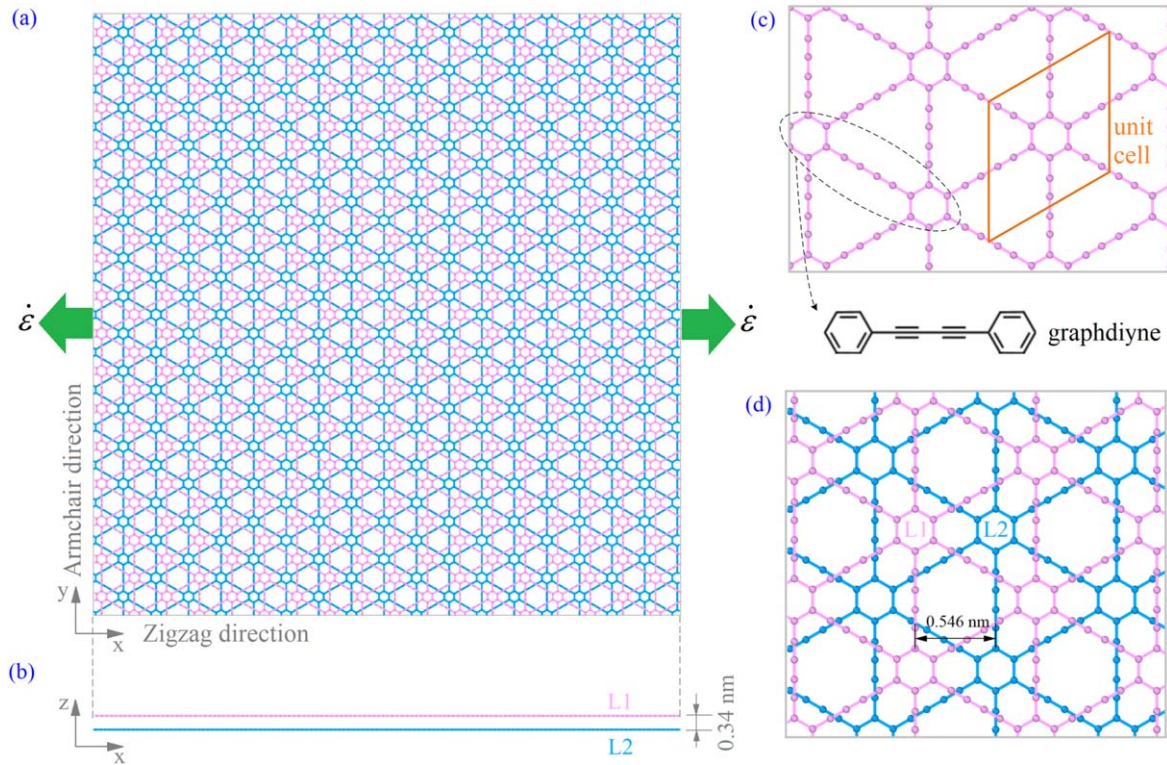
Figure 1. Schematic of a bilayer γ-graphdiyne (γ-BGDY) sheet geometry in an AB stacking order. (a) Top view and (b) side view of γ-BGDY with dimensions of 14.73 nm (*x*) by 15.12 nm (*y*) and an interlayer gap of 0.34 nm (*z*). The two layers are labeled as L1 (pink color) and L2 (blue color). (c) Unit cell and atomistic structure of γ-GDY. (d) Relative position of the top layer (L1) and the bottom layer (L2) stacking in AB mode in the *xy*-plane.

of the model along the loading direction could be expressed as $L(t) = L_0[1 + \dot{\varepsilon}(t - t_0)]$, where $L(t)$ and L_0 are the current and initial lengths at the time of t and t_0, respectively.

Prior to loading, the initial configuration of the nanostructure was modified by minimizing its potential energy with the steepest descent method and equilibrated in the NPT ensemble (constant number of atoms, constant pressure, and constant temperature) under a specific temperature and zero pressure for 1000 ps with a timestep of 0.5 fs. Thereafter, uniaxial tensile strains were applied to the γ-BGDY model by changing the length of the model along the loading direction at a constant strain rate. In the tensile process, the NVT ensemble (constant number of atoms, constant volume, and constant temperature) was adopted. During the simulations, temperatures were specified between 1 and 1000 K using a Nose–Hoover thermostat [39, 40]. Furthermore, when calculating the virial stress of the system along the loading direction, the thickness of the γ-BGDY model was assumed to be a constant of 6.8 Å.

In addition to the temperature effect, we studied the effect of loading direction (armchair and zigzag) and loading strain rate (varying from 0.005% ps^{-1} to 0.25% ps^{-1}) on the tensile properties of γ-BGDY. The effects of both loading direction and strain rate are less significant than that of temperature, and the fracture mechanism remains unchanged (see section S1 and section S2 in supplementary materials). Herein, we mainly analyze the uniaxial tensile properties along the zigzag direction with a strain rate of 0.05% ps^{-1} at different temperatures.
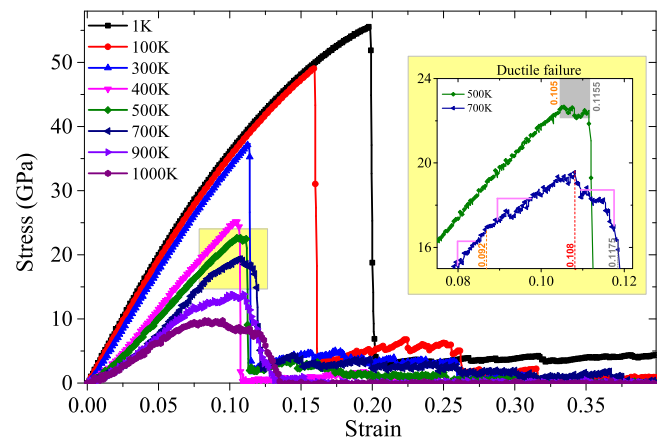
Figure 2. Stress–strain relations of γ-BGDY along the zigzag direction at different temperatures.

3. Temperature effect on the tensile properties of γ-BGDY

Figure 2 illustrates the stress–strain diagrams of the γ-BGDY system stretched at various temperatures. When the temperature is below 400 K, γ-BGDY first exhibits approximately linear elastic behavior, followed by a sharp drop of stress soon after the peak value, which is regarded as an abrupt brittle cleavage. When the temperature reaches 500 K, the stress–strain responses show that γ-BGDY exhibits ductile behavior. For example, the stress–strain curve at 500 K enters
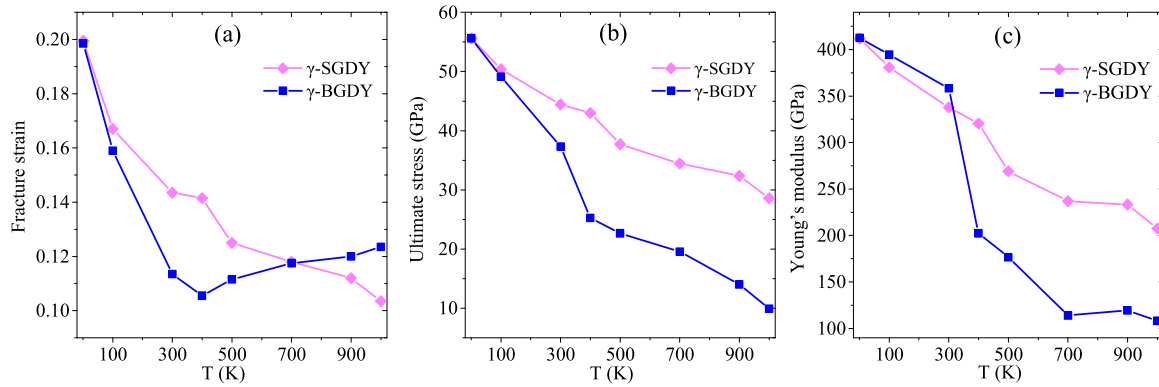
Figure 3. Temperature effect on the (a) fracture strain, (b) ultimate stress, and (c) Young's modulus of γ-SGDY and γ-BGDY.

a yield plateau in the strain interval of 0.105 and 0.1115, during which the strain continuously increases while the stress only fluctuates slightly near 22.41 GPa (see the inset curve in figure 2). After the yield plateau, the stress decreases quickly, indicating failure of the material. Hence, γ-BGDY undergoes a brittle-to-ductile transition at a critical temperature of approximately 500 K. Additional calculations were conducted at temperatures between 400 and 500 K. The results reveal that the critical temperature is approximately 450 K (figure S4). Besides, in a similar bilayer graphene system, the brittle-to-ductile transition has not been observed (figure S5).

Comparing these curves beyond the critical temperature indicates that they become more complicated at higher temperatures. When the temperature increases to 700 K, the stress increases again but at a lower rate after reaching the yielding point at the strain of 0.092 and reaches its peak value of 19.56 GPa at the strain of 0.108. Then, the stress decreases slowly for a short period before a final sharp drop at a tensile strain of 0.1175. Furthermore, the yield point appears earlier and the duration between the yield point and the final sharp drop point becomes longer at higher temperatures owing to the more complex deformation processes.

To better understand the temperature-dependent mechanical properties of γ-BGDY, we investigated its fracture strain, ultimate stress, and Young's modulus and compared them with those of γ-SGDY. Herein, the fracture strain is defined as the strain at which a destructive crack appears, the ultimate stress is determined as the peak stress in the stress–strain curve, and the Young's modulus is measured as the slope of the linear stage of the stress–strain curve.

From figure 3, the rupture strain, peak stress, and Young's modulus of γ-SGDY decrease monotonically with increasing temperature. A similar phenomenon was observed in testing other single-layer graphyne materials [41]. This is because higher temperatures mean stronger thermal vibrations of the carbon atoms, and less external energy is required for the breakage of the C–C bonds in the system. However, this condition changes in the γ-BGDY system. As shown in figure 3(a), with increasing temperature, the fracture strain of γ-BGDY decreases first before reaching the critical brittle-to-ductile transition temperature and then increases with temperature. This phenomenon can be explained by introducing a unique

interlayer cooperative deformation mechanism at high temperatures, which will benefit the application of γ-BGDY in bearing large deformation.

Moreover, the peak stress and the Young's modulus of γ-BGDY decrease continuously with temperature. In figure 3(b), the bearing capacity of γ-BGDY drops suddenly as the ambient temperature exceeds 300 K and is much lower than that of γ-SGDY. This is because once the temperature reaches 300 K, the microstructural rearrangements, such as newly formed interlayer bonds and ternary rings, appear between the unsaturated carbon atoms on diacetylenic linkages from L1 and L2 in the well-relaxed γ-BGDY system (figure S6). These rearrangements break the originally perfect crystal structure of γ-GDY and further cause severe stress concentration during tension. Therefore, compared with γ-SGDY, the γ-BGDY system breaks in advance (i.e. the bearing capacity of γ-BGDY is weakened).

In figure 3(c), when stretched below 300 K, the Young's moduli of γ-BGDY are slightly higher (∼5%) than that of γ-SGDY. A similar phenomenon was found in the bilayer graphene system [42], which was attributed to the van der Waals interaction between adjacent layers. Then, the Young's modulus first falls sharply and then becomes less sensitive to temperature owing to the microstructural evolutions within the γ-BGDY system involving in-plane defects and out-of-plane wrinkles at high temperatures.

From figure 3, it is also found that the mechanical properties of γ-GDY, i.e. the fracture strain, peak stress, and Young's modulus, are sensitive to the layer number. It is worth noting that the mechanical properties of multilayer graphene systems are insensitive to the layer number [42, 43]. Such difference can be explained by the different atomic structures and deformation mechanisms between γ-GDY and graphene.

Three typical snapshots of γ-BGDY with either brittle (1 K) or ductile (500 K) deformations are depicted in figure 4. In each case, the first snapshot represents the initial configuration of the well-relaxed γ-BGDY before stretching while the second and third snapshots denote the morphologies just before and after the fracture strain, respectively.

Comparing the two configurations at strains of 0 and 0.1985 shown in figure 4(a), we found that the γ-BGDY stretched at 1 K mainly undergoes a regular deformation without
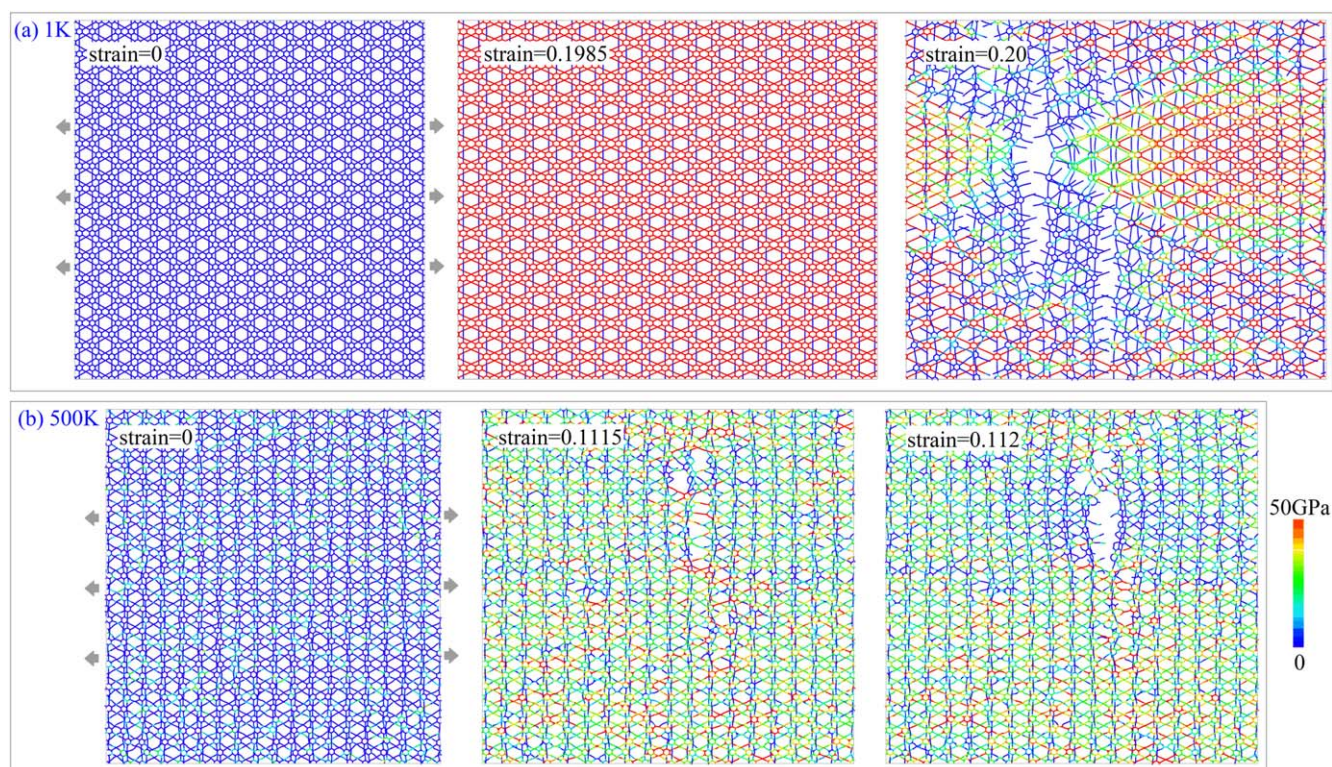
Figure 4. Snapshots of the deformed γ-BGDY systems under tension along the zigzag direction. (a) Configurations under 1 K at strains of 0.0, 0.1985, and 0.20, respectively. (b) Configurations under 500 K at strains of 0.0, 0.1115, and 0.112, respectively. Atoms are colored by the atomic-level stress component along the loading direction.

apparent rearrangement of the bond structure, corresponding to the nonlinear elastic stress–strain behavior shown in figure 2. As the strain increases to 0.20 (figure 4(a)), the destructive crack expands rapidly with a relatively smooth surface, indicating the occurrence of brittle fracture of γ-BGDY at low temperatures. The complete failure process of the γ-BGDY system stretched at 1 K is illustrated in Movie 1.

By contrast, the situation is considerably different when the γ-BGDY system is stretched at temperatures above the critical value of the brittle-to-ductile transition. In figure 4(b), structural reconstructions either in the plane or out of the plane occur in the well-equilibrated γ-BGDY system at 500 K. From the three snapshots in figure 4(b), the atoms in either L1 or L2 rearrange themselves obviously, which induces a nonuniform stress distribution and low bearing capacity in the stress–strain relationship. After the utmost rearrangement of atoms (i.e. at the strain of 0.112), γ-BGDY is torn apart with a rugged fracture surface, which directly reduces stress (Movie 2).

4. Microscopic deformation mechanism of temperature-dependent mechanical properties of γ-BGDY

The temperature-dependent brittle-to-ductile transition that appeared in γ-BGDY has been found in other low-dimensional nanomaterials, such as single-layer α-graphyne nanotubes [35], multilayer α-graphyne nanoscrolls [21], carbon nanotubes with Stone–Wales defects [44], and multilayer

black phosphorene nanoribbons [45]. However, their microscopic deformation mechanisms must be different owing to the apparent differences in the bonding and configuration. Herein, the atomic-level structural evolutions and fracture processes for brittle and ductile modes at different temperatures are analyzed to reveal the deformation mechanism of the brittle-to-ductile transition of γ-BGDY.

4.1. The brittle fracture of γ-BGDY without structural rearrangement at 1 K

When the temperature is below 300 K (e.g. 1 K), the thermal fluctuation of the atoms in γ-BGDY is weak. Therefore, as shown in figure 5(a1), L1 and L2 maintain their nearly perfect crystal structures in the well-relaxed γ-BGDY system. During tension, even though the carbon atoms in the diacetylenic chains are highly unsaturated, obvious microstructural evolution (particularly for the interlayer) is not observed in the stretched γ-BGDY system (see the snapshots shown in figure 5(a2)-(a3)). Hence, a smooth nonlinear elastic stress–strain response is exhibited at 1 K (figure 2).

At the strain of 0.1985, the system gets its ultimate strength of 55.6 GPa. With the strain increasing to 0.1990, the crack initiates from the top layer L1 due to the stress concentration (see the snapshots shown in figures 5(a4) and S7). As the tension goes on, the crack keeps expanding in the top layer. Meanwhile, the bottom layer L2 still bears the loading until it breaks at the strain of 0.1995 (see the snapshots shown in figures 5(a5) and S7). After that, the crack propagates in both layers and the system ruptures directly (Movie 1).
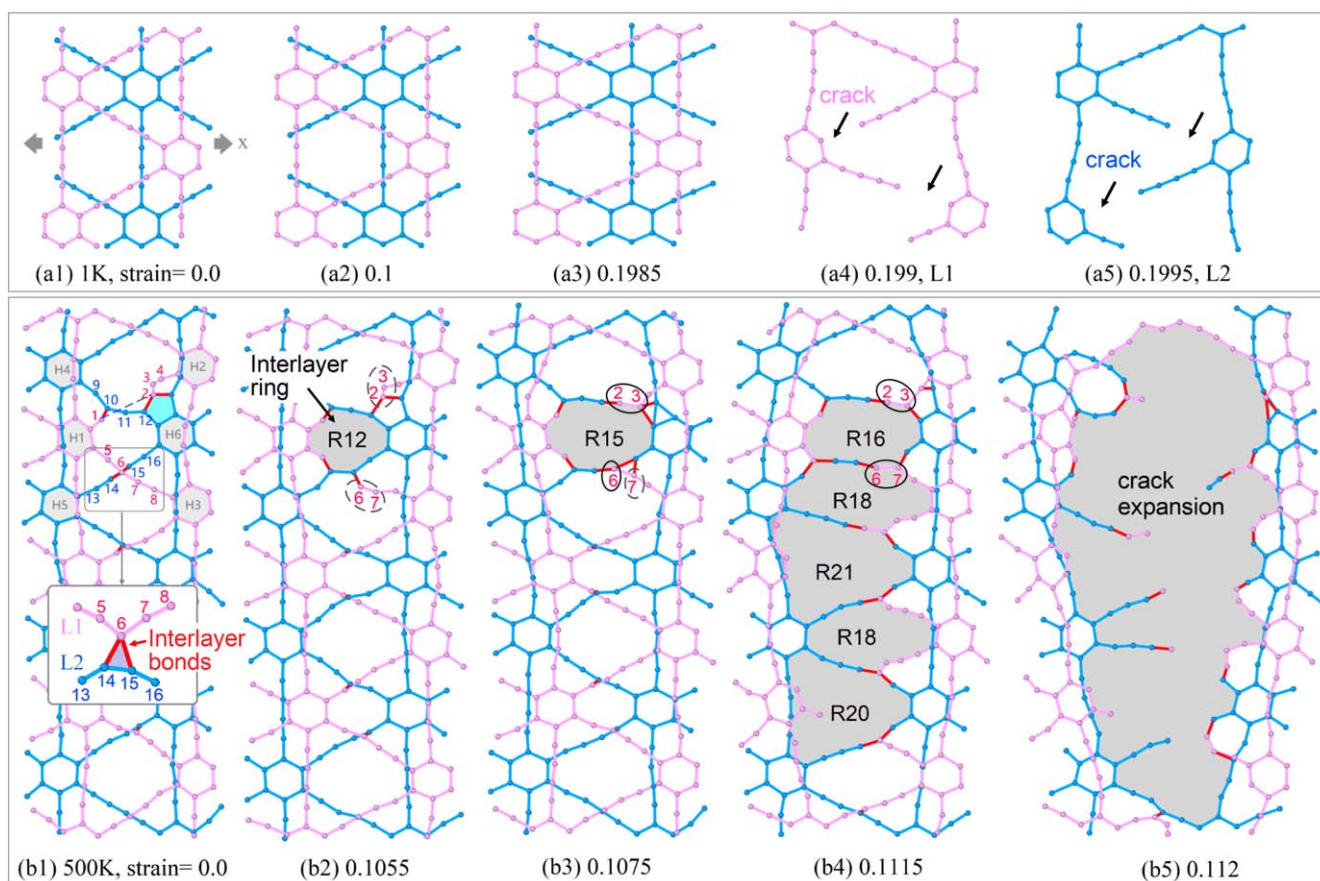
Figure 5. Representative microstructural evolutions of the γ-BGDY system when stretched along the zigzag direction at (a) 1 K and (b) 500 K. In (a), only stretched bonds are observed before the final brittle fracture. In (b), carbon atoms on four diacetylenic chains from neighboring layers are numbered from 1 to 16. The covalent carbon bonds generated between L1 and L2 are highlighted in red, and the related interlayer carbon rings are shown in gray.

Furthermore, the bond breakage always happens first in the single bonds either in L1 or L2 owing to the weaker strength of the single bond than that of the triple or aromatic bonds inside γ-GDY, which agrees overall with the fracture characteristics of single-layer graphyne materials [46].

4.2. The ductile deformation of stretched γ-BGDY with frequent structural realignments at 500 K

Based on the aforementioned details, microstructure rebuilding based on bond breakage and generation starts to occur in the diacetylenic chains from neighboring layers in the well-equilibrated γ-BGDY samples at temperatures exceeding 300 K. The microstructural evolutions become more complex at higher temperatures. For example, as depicted in figure 5(b1), when the temperature increases to 500 K, the formation of new interlayer C–C bonds (highlighted in red, e.g. between atoms No.6 and No.14 from L1 and L2, respectively) and the breakage of original intralayer bonds (illustrated by blue dash lines, e.g. between atoms No.1 and No.2 from L1) occur in the system. Therefore, in addition to the original 6- and 18-membered in-plane carbon rings inside L1 and L2, several irregular *n*-membered rings ($n = 3, 5, 7, \ldots, 11, 12, \ldots$), such as the cyan pentagon in figure 5(b1), are introduced in the well-relaxed γ-BGDY

system. Meanwhile, L1 and L2 are tightly connected by covalent bonds (see the enlarged snapshot in figure 5(b1)), implying that their co-deformation ability is activated. This is because of the high chemical reactivity of unsaturated (sp^1-hybridized) carbon atoms in the diacetylenic chains and their drastic thermal fluctuations at high temperatures. Furthermore, as previously reported, the self-rearrangements and formation of polygonal structural defects can be easily activated at an elevated temperature even within the γ-SGDY sheet [23].

The configuration evolutions related to the plastic yield plateau that emerges at 500 K under uniaxial tension are given in figures 5(b2)–(b4). In this period, an upper-level interlayer cooperative deformation evolution between L1 and L2, i.e. the generation and expansion of large interlayer carbon rings, can be easily identified. When stretched to the strain of 0.1055 at 500 K, a 12-membered interlayer carbon ring (labeled 'R12' and gray structure in figure 5(b2)), which contains atoms from both the top and bottom layers, is formed through complex bond breakages (e.g. between atoms No.5 and No.6) and formations (e.g. between atoms No.5 and No.14) and the annihilations of the interlayer ternary rings (e.g. comprising atoms No.6, No.14, and No.15 shown in the enlarged snapshot in figure 5(b1)). Upon increasing the tensile load, the atoms nearby incorporate into this ring continuously and enlarge the ring. For example, atoms No.2,

No.3, and No.6 join in at the strain of 0.1075 (figure 5(b3)) while atom No.7 incorporates at the strain of 0.1115 (figure 5(b4)), which enables the 12-membered ring to finally evolve into a large 16-membered polygon. Another four 18/ 21/18/20-membered interlayer rings (figure 5(b4)) are generated successively via frequent interlayer cooperative rearrangements between L1 and L2 until the strain of 0.1115. From the afore-mentioned analysis, benefiting from these efficient rearrangements of microstructure at 500 K, interlayer carbon rings are generated and expanded successively, which further affords the plasticity of the stress–strain curve and the improvement of the overall ductility of the system.

Finally, when the strain reaches 0.1115, the large interlayer pores are fully expanded and have the lowest local bond density in the system. Therefore, with further loading, a crack originates near the large pores and propagates through them immediately (figure 5(b5), Movie 2).

Herein, a complete temperature-dependent deformation mechanism of the γ-BGDY system can be given. When stretched below 300 K, L1 and L2 deform separately with no apparent microstructure reconstruction and the crack expands in a brittle manner without restriction. When the temperature exceeds 300 K but is lower than the critical brittle-to-ductile transition value, microstructure reconstruction starts to appear inside the γ-BGDY system but is still insufficient to trigger the brittle-to-ductile transition. Only when the temperature exceeds the critical value of brittle-to-ductile transition, the accumulation of microstructure reconstruction in the form of large interlayer rings can induce plasticity in the stretched γ-BGDY system. Furthermore, Both the number and size of the interlayer rings increase with the temperature, which affords the increasing trend in its fracture strain in figure 3(a).

In addition, according to our previous report [21], one-dimensional multilayer α-graphyne nanoscrolls exhibit a brittle-to-ductile transition when subjected to uniaxial tension. One may notice that the related structural reconstruction also occurs in the acetylenic chains and a deep analysis of this characteristic has already been given. However, the microscopic deformation mechanisms of the brittle-to-ductile transitions of the two-dimensional γ-BGDY sheet and the one-dimensional multilayer α-graphyne nanoscroll are quite different owing to their bonding differences. The former is dominated by large interlayer rings, whereas the latter is mainly controlled by intralayer ternary rings.

5. Conclusion

Based on the uniaxial tension tests via the reactive MD simulations, the mechanical properties of (γ-BGDY) material, including fracture stress, fracture strain, and Young's modulus and corresponding microscopic deformation mechanisms were systematically investigated. The single-layer γ-graphdiyne (γ-SGDY) was considered for comparative purposes. Our simulation results show that the tensile properties of γ-BGDY are strongly dependent on temperature and exhibit an interesting brittle-to-ductile transition with increasing temperature. Unlike the monotonic decreasing trends associated with the mechanical

properties of γ-SGDY, for γ-BGDY, only the ultimate stress and Young's modulus decrease with temperature while its fracture strain first decreases with temperature before reaching the critical brittle-to-ductile transition value and then increases gradually. Owing to the severe thermal vibrations of the atoms located in diacetylenic chains at temperatures exceeding 300 K, an interlayer cooperative deformation mechanism based on frequent reconstruction is activated inside γ-BGDY, which should be responsible for the brittle-to-ductile transition and the enhanced deformability at high temperatures beyond the critical brittle-to-ductile transition value. Furthermore, the brittle-to-ductile transition of γ-BGDY and its microscopic mechanism are slightly affected by the loading direction and the loading rate. The present study should be very useful for the further design of γ-GDY in future applications, such as nanoelectronics.

Acknowledgments

Data availability statement

The data generated and/or analysed during the current study are not publicly available for legal/ethical reasons but are available from the corresponding author on reasonable request.

Compliance with ethical standards

The authors comply with the ethical rules for this journal.

Conflict of interest

The authors declare that they have no conflict of interest.

ORCID iDs

Bo Song ⓘ https://orcid.org/0000-0003-4561-3858
Chao Wang ⓘ https://orcid.org/0000-0002-3234-6917
Shaohua Chen ⓘ https://orcid.org/0000-0002-5277-453X

References

[1] Baughman R H, Eckhardt H and Kertesz M 1987 Structure-property predictions for new planar forms of carbon: layered phases containing sp2 and sp atoms *J. Chem. Phys.* **87** 6687–99

[2] Haley M M, Brand S C and Pak J J 1997 Carbon networks based on dehydrobenzoannulenes: synthesis of graphdiyne substructures *Angew. Chem. Int. Ed. Engl.* **36** 836–8

[3] Narita N *et al* 1998 Optimized geometries and electronic structures of graphyne and its family *Phys. Rev.* B **58** 11009–14

[4] Li G X *et al* 2010 Architecture of graphdiyne nanoscale films *Chem. Commun.* **46** 3256–8

[5] Liu R *et al* 2017 Graphdiyne filter for decontaminating lead-ion-polluted water *Adv. Electron. Mater.* **3** 1700122

[6] Pei Y 2012 Mechanical properties of graphdiyne sheet *Physica* B **407** 4436–9

[7] Zheng Q Y *et al* 2012 Structural and electronic properties of bilayer and trilayer graphdiyne *Nanoscale* **4** 3990–6

[8] Zhang H Y *et al* 2013 Graphdiyne: a promising anode material for lithium ion batteries with high capacity and rate capability *J. Appl. Phys.* **113** 044309

[9] Hui L *et al* 2018 Overall water splitting by graphdiyne-exfoliated and -sandwiched layered double-hydroxide nanosheet arrays *Nat. Commun.* **9** 5309

[10] Sun C Y *et al* 2022 Modulation of graphene and graphdiyne by metaln ($n = 1$–5) adsorption and nucleation and the effect on hydrogen evolution reaction *Appl. Surf. Sci.* **580** 152197

[11] Li B S *et al* 2020 Graphdiyne: a rising star of electrocatalyst support for energy conversion *Adv. Energy Mater.* **10** 2000177

[12] Kan X N *et al* 2020 Graphdiyne-Supported atomic catalysts: synthesis and applications *ChemPlusChem* **85** 2570–9

[13] Qiu H *et al* 2019 Graphynes for water desalination and gas separation *Adv. Mater.* **31** 1803772

[14] Malko D *et al* 2012 Competition for graphene: graphynes with direction-dependent dirac cones *Phys. Rev. Lett.* **108** 086804

[15] Hernandez S A and Fonseca A F 2017 Anisotropic elastic modulus, high poisson's ratio and negative thermal expansion of graphynes and graphdiynes *Diam. Relat. Mater.* **77** 57–64

[16] Hou J *et al* 2015 An analytical molecular mechanics model for elastic properties of graphyne-n *J. Appl. Mech.* **82** 094501

[17] Cranford S W, Brommer D B and Buehler M J 2012 Extended graphynes: simple scaling laws for stiffness, strength and fracture *Nanoscale* **4** 7797–809

[18] Georgantzinos S K and Siampanis S G 2021 Size-dependent elastic mechanical properties of γ-graphyne structures: a comprehensive finite element investigation *Mater. Des.* **202** 109524

[19] Xiao K L *et al* 2019 Nanoindentation of thin graphdiyne films: experiments and molecular dynamics simulation *Carbon* **144** 72–80

[20] Rouhi S and Pourmirzaagha H 2018 Molecular dynamics investigation of the mechanical behavior of multi-layered graphyne and its family under tensile loading *J. Mol. Graph. Modell.* **80** 299–312

[21] Yang B L *et al* 2022 Temperature-dependent brittle-ductile transition of α-graphyne nanoscroll and its micromechanism *Carbon* **191** 98–105

[22] Ahangari M G 2015 Effect of defect and temperature on the mechanical and electronic properties of graphdiyne: a theoretical study *Physica* E **66** 140–7

[23] Ma S Y *et al* 2016 High-temperature behavior of monolayer graphyne and graphdiyne *Carbon* **99** 547–55

[24] Ryota M *et al* 2017 Crystalline graphdiyne nanosheets produced at a gas/liquid or liquid/liquid interface *J. Am. Chem. Soc.* **139** 3145–52

[25] Plimpton S 1995 Fast parallel algorithms for short-range molecular dynamic *J. Comput. Phys.* **117** 1–19

[26] Stuart S J, Tutein A B and Harrison J A 2000 A reactive potential for hydrocarbons with intermolecular interactions *J. Chem. Phys.* **112** 6472–86

[27] Legoas S B *et al* 2003 Molecular-dynamics simulations of carbon nanotubes as gigahertz oscillators *Phys. Rev. Lett.* **90** 055504

[28] Song B *et al* 2019 Coupling effect of van der Waals, centrifugal, and frictional forces on a GHz rotation-translation nano-convertor *Phys. Chem. Chem. Phys.* **21** 359–68

[29] Zhao H, Min K and Aluru N R 2009 Size and chirality dependent elastic properties of graphene nanoribbons under uniaxial tension *Nano Lett.* **9** 3012–5

[30] Zhang C, Peng Z L and Chen S H 2014 Chirality-controlled carbon nanotubes fabricated by self-assembly of graphene nanoribbons *J. Phys. Chem.* C **118** 19477–83

[31] Shi J *et al* 2020 A GHz rotary nanoflake driven by diamond needles: a molecular dynamics study *Mater. Des.* **191** 108593

[32] Shi J, Cai K and Xie Y M 2018 Thermal and tensile properties of diamondene at finite temperature: a molecular dynamics study *Mater. Des.* **156** 125–34

[33] Cai K, Wang L and Xie Y M 2018 Buckling behavior of nanotubes from diamondene *Mater. Des.* **149** 34–42

[34] Yang Y L and Xu X M 2012 Mechanical properties of graphyne and its family-A molecular dynamics investigation *Comput. Mater. Sci.* **61** 83–8

[35] Zhang C *et al* 2021 Temperature-dependent brittle-ductile transition of α-graphyne nanotubes under uniaxial tension *Comput. Mater. Sci.* **187** 110083

[36] Wang S W *et al* 2017 Fracture behaviors of brittle and ductile 2D carbon structures under uniaxial tensile stress *Carbon* **111** 486–92

[37] Liu M X *et al* 2022 Strength and fracture behaviors of ultralong carbon nanotubes with defects *Carbon* **199** 300–17

[38] Shenderova O A *et al* 2000 Atomistic modeling of the fracture of polycrystalline diamond *Phys. Rev.* B **61** 3877–88

[39] Hoover W G 1985 Canonical dynamics: equilibrium phase-space distributions *Phys. Rev.* A **31** 1695–7

[40] Nosé S 1984 A unified formulation of the constant temperature molecular dynamics methods *J. Chem. Phys.* **81** 511–9

[41] Zhang Y Y *et al* 2014 Temperature and strain-rate dependent fracture strength of graphynes *J. Phys. D: Appl. Phys.* **47** 425301

[42] Zhang Y Y and Gu Y T 2013 Mechanical properties of graphene: effects of layer number, temperature and isotope *Comput. Mater. Sci.* **71** 197–200

[43] An M R *et al* 2018 The effect of defects on the fracture behavior of trilayer graphene *Superlattices Microstruct.* **123** 172–82

[44] Nardelli M B, Yakobson B I and Bernholc J 1998 Brittle and ductile behavior in carbon nanotubes *Phys. Rev. Lett.* **81** 4656–9

[45] Wang L and Cai K 2018 Brittle-to-ductile transition in fracture of few-layered black phosphorus ribbons under uniaxial stretching *Comput. Mater. Sci.* **144** 210–5

[46] Zhang Y Y, Pei Q X and Wang C M 2012 Mechanical properties of graphynes under tension: a molecular dynamics study *Appl. Phys. Lett.* **101** 081909